

# NASICON Catalysts with Composition $\text{Na}(\text{Cs})_{1-2x}\text{M}_x\text{Zr}_2(\text{PO}_4)_3$ for Transformations of Aliphatic Alcohols

I. I. Mikhailenko<sup>a</sup>, \*, A. I. Pylina<sup>a</sup>, and E. I. Knyazeva<sup>a</sup>

<sup>a</sup>*Peoples' Friendship University of Russia, Moscow, 117198 Russia*

\**e-mail: mikhailenko\_ii@pfur.ru*

Received July 22, 2019; revised February 7, 2020; accepted June 11, 2020

**Abstract**—The activity of solid electrolytes from the family of  $\text{Na}(\text{Cs})\text{—M}_x\text{—Zr}$  phosphates (N-ZP and C-ZP) with dopant ions  $\text{M}^{+2} = \text{Co}^{+2}$  and  $\text{Ni}^{+2}$  synthesized by the sol–gel method is studied in the gas-phase transformations of isopropanol and isobutanol. It is found that the amount of  $\text{M}^{+2}$  and its nature, as well as the direction of a change in the catalyst temperature (heating or cooling in the range of 473–693 K), affects the activity of M-N-ZP and M-C-ZP. In the transformation of isopropanol, hysteresis of the acetone yield, counter-clockwise (type I) for Co-N-ZP and clockwise (type II) for Ni-N-ZP, is observed in the heating–cooling cycles. An increase in the activity of Co-N-ZP in the cooling mode (type I) is related to a rise in the apparent activation energy of alcohol dehydrogenation under conditions of the formation of new catalytically active sites in the form of a  $\text{Co}^{+2}\text{—Zr}^{+4} \rightarrow \text{Co}^{+3}\text{—Zr}^{+3}$  ion pair with the oxidized form of M and the reduced form of Zr. Type I hysteresis of the total alcohol conversion is observed in the transformations of isobutanol to olefin and aldehyde over Co(Ni)-C-ZP. The hysteresis is associated with a decrease in the activation energy of alcohol dehydrogenation. The main reaction over the Co(Ni)-C-ZP catalysts is the dehydration of alcohol with an increase in the activation energy of the reaction upon cooling, for example, by 53 kJ/mol for  $\text{Ni}_{0.25}\text{—C-ZP}$ .

**Keywords:** sol–gel synthesis, complex zirconium orthophosphates, dopant cations, nickel, cobalt, isopropanol, isobutanol, dehydrogenation and dehydration of alcohol, catalytic activity, thermal hysteresis

**DOI:** 10.1134/S0965544120100096

Catalytic dehydrogenation of low-molecular-weight aliphatic alcohols is a simple method for obtaining carbonyl compounds and hydrogen. It is easy to vary the direction of transformation (dehydrogenating and dehydrating functions of the catalyst) by changing the composition of the catalyst.

Complex zirconium orthophosphates with the framework structure, which belong to solid cationic electrolytes with the NASICON structure of the general formula  $\text{MA}_2(\text{PO}_4)_3$ , where M are the conducting ions of alkaline metals and A are the ions of 3d-transition metals, attract considerable attention of catalytic chemists. This is associated with the fact that modification of the catalyst aimed at improvement of its catalytic activity and change in the selectivity of the process may involve introduction of various cations into the phosphate composition through replacement of both the framework ion A and the conducting ions M without violation of the framework structure. Rhombohedral, rhombic, monoclinic, and cubic structures are possible for NASICON electrolytes. For basic orthophosphate  $\text{NaZr}_2(\text{PO}_4)_3$  the main structure is rhombohedral, which represents  $\text{PO}_4$  tetrahedra and  $\text{ZrO}_6$  octahedra with the vertex contacts between the polyhedra united into a framework. The preparation, crystallochemistry features, and application of com-

plex orthophosphates were considered in [1–4], and the data on the catalytic activity of such materials in vapor-phase reactions involving alcohols were reported in [5–11].

The aim of this work is to investigate effect of the partial replacement of conducting sodium or cesium cations with nickel and cobalt cations on the activity of  $\text{Na}(\text{Cs})$  zirconium phosphate synthesized by the sol–gel method in the transformations of isopropanol and isobutanol under temperature increase–decrease cycles in the temperature range of 473–693 K. This work continues the research topics of [9–11].

## EXPERIMENTAL

### *The Sol–Gel Synthesis of Ni(Co)–N-ZP*

The initial substances were  $\text{ZrO}_2$  (Acros Organics),  $\text{H}_3\text{PO}_4$ ,  $\text{NaCl}$ ,  $\text{NiCl}_2 \cdot 2\text{H}_2\text{O}$ , and  $\text{CoCl}_2 \cdot 6\text{H}_2\text{O}$  (all of reagent grade). The stoichiometric amounts of  $\text{NaCl}$  and  $\text{ZrO}_2$  aqueous solutions of predissolved in  $\text{HCl}$  to avoid hydrolysis were poured together under continuous stirring at room temperature, and  $\text{NiCl}_2$  or  $\text{CoCl}_2$  was slowly added dropwise a  $\text{H}_3\text{PO}_4$  solution according to the stoichiometry. The gel formed upon heating was dried at 80 and 110°C and subjected to thermal

**Table 1.** Texture, elemental composition of the surface, and structural characteristics of the initial samples of  $\text{Na}_{1-2x}\text{M}_x\text{Zr}_2(\text{PO}_4)_3$  with Ni and Co

$M_x$	Dispersity			Unit cell parameters and volume		
	specific surface area, $\text{m}^2/\text{g}$	pore volume, $\text{cm}^3/\text{g}$	pore diameter, $\text{\AA}$	$a = b$ , $\text{\AA}$	$c$ , $\text{\AA}$	$V$ , $\text{\AA}^3$
$\text{Ni}_{0.125}\text{-NZP}$	2.4	0.0252	267	8.801	22.791	547
$\text{Ni}_{0.25}\text{-NZP}$	1.5	0.0359	276	8.835	22.83	393
$\text{Co}_{0.125}\text{-NZP}$	1.2	0.0309	214	8.798	22.75	476
$\text{Co}_{0.25}\text{-NZP}$	1.4	0.0205	256	8.788	22.82	526
$M_x$	at % (X-ray photoelectron spectroscopy data)			Unit cell parameters and volume		
	Cs	M	Zr	$a = b$ , $\text{\AA}$	$c$ , $\text{\AA}$	$V$ , $\text{\AA}^3$
$\text{Ni}_{0.15}\text{-CZP}$				8.569	24.938	1585.9
$\text{Ni}_{0.25}\text{-CZP}$	4.2 (2.8)	3.7 (1.4)	12.1 (11.3)	8.569	24.938	1585.8
$\text{Co}_{0.15}\text{-CZP}$				8.575	24.958	1589.3
$\text{Co}_{0.25}\text{-CZP}$	4.2 (2.8)	5.4 (1.4)	12.1 (11.3)	8.571	24.948	1587.2

Bracketed figures in italics refer to the stoichiometric concentration of the element.

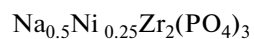
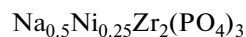
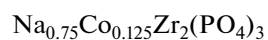
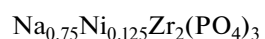
treatment at 600 and 800°C for 8 h accompanied by grinding at each stage.

#### The Sol–Gel Synthesis of Ni(Co)-CZP

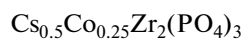
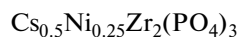
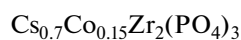
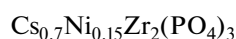
The initial substances were  $\text{ZrOCl}_2 \cdot 8\text{H}_2\text{O}$  (Acros Organics),  $\text{H}_3\text{PO}_4$ , CsBr,  $\text{NiCl}_2$ , and  $\text{CoCl}_2$  (all of reagent grade).  $\text{H}_3\text{PO}_4$  was added dropwise in a mixture of the weighed portions of solid salts according to stoichiometry. The resulting gel was dried for three days with regular grinding, the ground samples were placed into a drying oven at 300°C for 4 h, after which they were subjected to calcination at 600°C for 6 h.

The obtained samples were polycrystalline powders with characteristic pale green (Ni) and lilac (Co) colors:

#### M-NZP



#### M-CZP



The phase and chemical compositions, specific surface area, and porosity of M-NZP and M-CZP were studied by X-ray powder diffraction analysis (Rigaku Ultim IV, DRON-7), scanning ion–electron spectroscopy (Quanta 200 3D), low-temperature nitrogen adsorption (TriStar 3000, ASAP 2020-MP Micromeritics), and X-ray photoelectron spectroscopy (XPS) (Axis Ultra, Kratos Analytical).

The catalytic activity of complex zirconium phosphates in the transformations of isopropanol and isobutanol was tested on a flow-type unit followed by the chromatographic analysis of substances (helium as

a carrier gas, a flame ionization detector, and column packed with a Porapak-Q sorbent). The feed rate of a helium + alcohol mixture to the microreactor was  $1.2 \text{ L h}^{-1}$ . The weight of the catalyst with a 1–2-mm-thick catalyst bed on a porous filter was 30 mg. The sample was pre-exposed in a helium flow at 673 K for 1 h followed by a slow decrease in the temperature of the reactor to 373 K. The temperature dependences of the yield of the products were obtained in the modes of increasing and decreasing temperature provided that the stationary activity of the catalyst was reached at each temperature, which took 15–20 min. For the temperature range, in which alcohol conversion did not exceed 50%, the experimental activation energies of dehydrogenation ( $E_a^{\text{C=O}}$ ) and dehydration ( $E_a^{\text{C=C}}$ ) of alcohol were calculated from the Arrhenius dependences of the yield of reaction product  $N$

## RESULTS AND DISCUSSION

The data on the porosity, specific surface area, and crystal structure of M-NZP for  $\text{Na}_{0.75}\text{M}_{0.125}\text{Zr}_2(\text{PO}_4)_3$  and  $\text{Na}_{0.5}\text{M}_{0.25}\text{Zr}_2(\text{PO}_4)_3$  with  $M = \text{Co}$  and  $\text{Ni}$  are presented in Table 1. The rhombohedral modification of the NASICON structure, which is characteristic for the family of sodium zirconium phosphates (NZP), was confirmed by fact that the positions and relative intensity of the maxima of the diffraction patterns coincided with the published data.

Ceramic materials have a small specific surface area  $S_{\text{sp}}$ , and the sample with  $\text{Ni}_{0.125}$  is characterized by the highest surface area in the M-NZP series. In terms of pore sizes (210–280 Å) NZP belong to mesoporous systems. The conductance channels filled with Na, Cs, Ni, and Co cations have a size of 8–10 Å, and, according to the published data, such pores are appar-

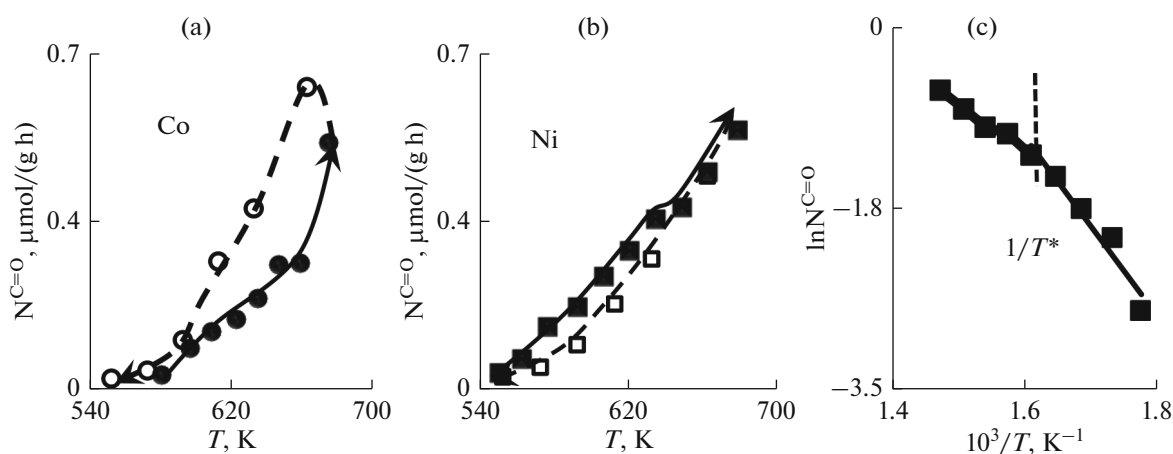


**Fig. 1.** (a, b) Temperature dependences of the yield of acetone over the  $\text{Na}_{0.75}\text{M}_{0.125}\text{Zr}_2(\text{PO}_4)_3$  catalysts in the mode of (solid lines) increasing and (dashed lines) decreasing temperature and (c) the Arrhenius dependence for Ni-NZP.

ently inaccessible to the sorption/desorption of nitrogen. The unit cell volume  $V$  decreases by 28% with an increase in the concentration of Ni, while Co-NZP it increases by  $\sim 10\%$ , which is within the accuracy of determination of  $V$ . The X-ray powder diffraction analysis showed that all the Ni(Co)-NZP samples contain small amounts of  $\text{ZrO}_2$  and  $\text{ZrP}_2\text{O}_7$ .

According to X-ray analysis,  $\text{Cs}_{0.7}\text{M}_{0.15}\text{Zr}_2(\text{PO}_4)_3$  and  $\text{Cs}_{0.5}\text{M}_{0.25}\text{Zr}_2(\text{PO}_4)_3$  have a rhombohedral crystal lattice like  $\text{CsZr}_2(\text{PO}_4)_3$ . The crystal lattice parameters of triple phosphates (Table 1) are close to the lattice parameters of the double phosphate ( $a = 8.581 \pm 0.001 \text{ \AA}$ ,  $c = 24.973 \pm 0.005 \text{ \AA}$ ,  $V = 1592.3 \pm 0.4 \text{ \AA}^3$ ) but with decreased values of  $a$ ,  $c$ , and  $V$ . A linear change in the unit cell parameters of Co-CZP with an increase in the concentration of the dopant ion was discussed in [11]. For triple phosphates the specific surface area and the pore volume are  $4.1 \text{ m}^2/\text{g}$  and  $0.0002 \text{ cm}^3/\text{g}$  for  $\text{Cs}_{0.7}\text{M}_{0.15}\text{Zr}_2(\text{PO}_4)_3$  and  $1.5 \text{ m}^2/\text{g}$  and  $0.002 \text{ cm}^3/\text{g}$  for  $\text{CsZr}_2(\text{PO}_4)_3$ , respectively.

The values of the binding energy of all elements obtained from the XPS spectra of the samples from the Ni(Co)-CZP series corresponded to the phosphate formula. The atomic ratio of oxygen to phosphorus O/P was overestimated against the stoichiometric ratio; it was 6 and 5.6 for Co-CZP and Ni-CZP, respectively. This finding suggests an excessive concentration of the oxygen of the phosphate groups on the surface. The surface concentration of Cs is increased 1.5-fold and the surface concentration of dopant ions is increased 2.6-fold (Ni) and 3.8-fold (Co) in comparison with the stoichiometry of the phosphate (Table 1). The concentration of Zr corresponds to the stoichiometric concentration.

Over Na–Co(Ni) zirconium phosphates (Co-NZP and Ni-NZP) only the dehydrogenation of isopropanol proceeds, and the double phosphate  $\text{NaZr}_2(\text{PO}_4)_3$  demonstrates no catalytic activity. A change in the

amount of the formed acetone for the catalysts with the concentration of cobalt and nickel  $x = 0.125$  in the heating–cooling cycle is presented in Figs. 1a and 1b.

Only in the case of the Co-containing sample activity was higher upon decrease in temperature compared with the mode of increasing temperature; i.e., a counter-clockwise thermal hysteresis (type I hysteresis) was observed. A small decrease in the values of  $N^{C=O}$  with decreasing temperature (type II hysteresis) was recorded for the Ni-containing sample.

A similar activity testing was performed for the number of samples with  $x = 0.25$ . In the case of  $\text{Co}_{0.25}\text{-NZP}$ , the type of hysteresis changed while for  $\text{Ni}_{0.25}\text{-NZP}$  the clockwise hysteresis was more pronounced.

A distinctive feature of sodium zirconium phosphates is that the energetically favorable position of the ion in the conductance channel changes at 573–593 K. This factor and its role in the dehydrogenating ability of M-NZP were discussed in [10]. In the temperature range of  $T^* \sim 593\text{--}613 \text{ K}$  in the Arrhenius dependences of the yield of acetone over the Ni-NZP catalysts a break is observed with a decrease in the slope of straight lines  $\ln N^{C=O} - T^{-1}$  (Fig. 1c). This is evidence that the catalytic reaction is sensitive to the transition of cation in the NZP conductance channel from position M1 to position M2. The break in the dependences  $\ln N^{C=O} - T^{-1}$  is repeated under the mode of decreasing temperature of the catalyst, which indicates the reversibility of the M1–M2 transition with low ( $T > T^*$ ) and high ( $T < T^*$ ) experimental activation energies of isopropanol dehydrogenation  $E_a$  being preserved.  $\text{Co}_{0.125}\text{-NZP}$  does not have such a characteristic feature, while for  $\text{Co}_{0.25}\text{-NZP}$  it is slightly pronounced, which suggests that cobalt occurs in the special state.

The yield of acetone normalized to the unit surface of M-NZP samples, that is, the specific activity of the

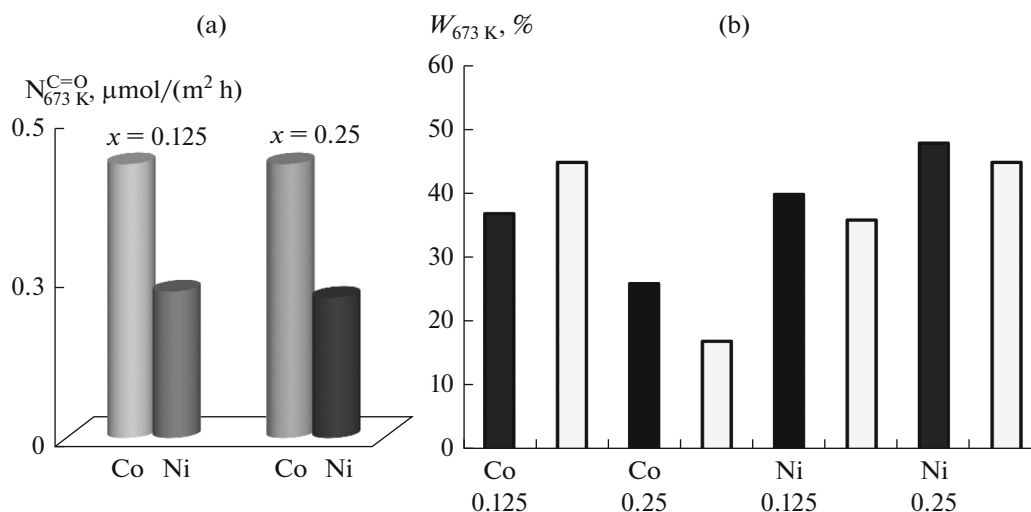


**Fig. 2.** (a) Yield of acetone normalized to the unit surface (the heating mode) and (b) degree of transformation of isopropanol over the  $\text{Na}_{(1-2x)}\text{M}_x\text{Zr}_2(\text{PO}_4)_3$  catalysts, where  $\text{M} = \text{Co}$  and  $\text{Ni}$ , in the mode of heating (dark columns) and cooling (light columns).

catalysts, does not depend on the concentration of  $\text{M}$ ; it is higher in the case of  $\text{Co-NZP}$  (Fig. 2a). The depth of the transformation (conversion) of isopropanol  $W$  increases in the mode of decreasing temperature for  $\text{Co}_{0.125}\text{-NZP}$  (Fig. 2b), while for  $\text{Co}_{0.25}\text{-NZP}$  this value decreases. The conversion of alcohol over the  $\text{Co}_{0.25}\text{-NZP}$  catalyst is lower than that over  $\text{Co}_{0.125}\text{-NZP}$ . This feature distinguishes the samples with  $\text{Co}$  from the samples with  $\text{Ni}$ . Upon cooling of the  $\text{Ni-NZP}$  catalysts conversion decreased.

Table 2 presents the yields of the product  $N$  at a temperature of 593 K, which is in the region of the  $\text{M1-M2}$  transition and the values of  $E_a$ . It follows from the analysis of  $\Delta N$  that a large counter-clockwise hysteresis of the acetone yield (the “plus” sign in front of  $\Delta N = N_{\downarrow} - N_{\uparrow}$  in Table 2) is characteristic for the  $\text{Co}_{0.125}\text{-NZP}$  catalyst; for the corresponding nickel catalyst, clockwise hysteresis (the “minus” sign).

Let us analyze a change in the Arrhenius parameters of dependences  $\ln N^{\text{C=O}} - T^{-1}$  for the dehydrogenation reaction of isopropanol (the values of  $\Delta E_a$  and  $\Delta \ln N_0$ ). The yield of the product is the rate of reaction of alcohol dehydrogenation, which is equal or directly proportional to the rate constant of the reaction  $K$  in the absence of diffusion limitations; therefore,  $N_{\downarrow}/N_{\uparrow} \approx K_{\downarrow}/K_{\uparrow}$ . Taking the logarithm of  $N_{\downarrow}/N_{\uparrow}$ , we obtain the expression

$$\ln(N_{\downarrow}/N_{\uparrow}) = \Delta \ln N_0 - (RT)^{-1} \Delta E_a, \quad (1)$$

from which it follows that the thermal hysteresis may be related to a change in both the apparent activation energy of the reaction  $\Delta E_a = E_{a\downarrow} - E_{a\uparrow}$  and the logarithm of the preexponential factor  $\Delta \ln N_0 = \ln N_{0\downarrow} - \ln N_{0\uparrow}$  (Table 1). The accuracy of determination of  $E_a$  is  $\pm 5-7$  kJ/mol; therefore, the values of  $\Delta E_a$  are negligible within 10 kJ/mol. Expression (1) can be written as the equation

**Table 2.** Hysteresis parameters for the  $\text{Na}_{(1-2x)}\text{M}_x\text{Zr}_2(\text{PO}_4)_3$  catalysts: the change in the yield of acetone in the cooling–heating cycle ( $\Delta N$ , %) at  $T \sim T^*$ , apparent activation energy of formation of acetone ( $E_a$ ) in the mode of heating (numerator) and cooling (denominator), and changes in the activation energy and logarithm of the preexponential factor

$\text{M}_x$	$\Delta N_{593\text{ K}} \%$	$E_a \uparrow / E_a \downarrow$		$\Delta E_a$ , kJ/mol		$\Delta \ln N_0$	
		$T < T^*$	$T > T^*$	$T < T^*$	$T > T^*$	$T < T^*$	$T > T^*$
$\text{Co}_{0.125}$	+90	70/96		+26		+ 5.5	
$\text{Co}_{0.25}$	−30	93/60	67/67	−33	0	−5.5	+1
$\text{Ni}_{0.125}$	−57	72/91	36/61	+19	+25	+3.3	+4.4
$\text{Ni}_{0.25}$	0	83/114	44/64	+31	+20	+6.2	+3.7

$$\ln(N\downarrow/N\uparrow) = \Delta \ln N_0 - (RT)^{-1}(\alpha Q\uparrow - \alpha' Q\downarrow), \quad (2)$$

because according to the linearity ratio

$$E_a = E_a^0 - \alpha Q, \quad (3)$$

where  $E_a^0$  is the true activation energy of the reaction,  $Q$  is the heat of adsorption of alcohol, and  $\alpha$  is the contribution of heat to  $E_a$ .

The growth in activity upon cooling the catalyst—the counter-clockwise hysteresis—may be associated with both a decrease in  $E_a$  ( $\Delta E_a < 0$ ) and an increase in the preexponential factor ( $\Delta \ln N_0 > 0$ ). Both factors act simultaneously with the predominance of one over another. The opposite type of hysteresis is also possible with a similar-in-sign change in  $E_a$  and  $\ln N_0$ , like in the case of  $\text{Co}_{0.125}$ -NZP and  $\text{Ni}_{0.125}$ -NZP catalysts. A significant growth in the activity of  $\text{Co}_{0.125}$ -NZP in the cooling mode is related to the increase in  $E_a$  and  $\ln N_0$  due to the involvement of new sites with a decreased heat of adsorption  $Q$  in the reaction, that is, to the strength of the bond of the alcohol with the catalyst. There is no break in the  $\ln N^{\text{C=O}}-T^{-1}$  dependences for  $\text{Co}_{0.125}$ -NZP. For the  $\text{Ni}_{0.125}$ -NZP catalyst with the clockwise hysteresis, which is sensitive to the M1–M2 transition, the result was similar to that for  $\text{Co}_{0.125}$ -NZP:  $\Delta E_a > 0$  and  $\Delta \ln N_0 > 0$  at  $T < T^*$  and  $T > T^*$ . The absence or a weak thermal hysteresis is possible in the case of the same contribution from the first and second summands of Eq. (1). An example of such a compensation is the dehydrogenation of isopropanol over  $\text{Ni}_{0.25}$ -NZP with the same character of change in  $E_a$  and  $\ln N_0$ .

The charge states of nickel and cobalt can change in the reducing medium of the alcohol dehydrogenation reaction. In terms of the oxidation–reduction mechanism of the reaction, in which the stage of reoxidation of M is treated as the limiting stage [5], it is difficult to explain the activity of  $\text{Ni}^{+2}$  and  $\text{Co}^{+2}$  by the negative value of the reduction potential<sup>1</sup>:  $-0.257$  V (Ni) and  $-0.27$  V (Co) for the reaction  $\text{M}^{+2} + 2e = \text{M}^0$ .

The reduction potential is positive  $E_r^0 = +1.39$  V only for  $\text{Co}^{+3} \rightarrow \text{Co}^{+2}$ . The appearance of the oxidized form of  $\text{Co}^{+3}$  in the composition of the catalytically active site of the reaction can be explained by formation of a bimetallic pair  $\text{Co}^{+2}-\text{Zr}^{+4} \rightarrow \text{Co}^{+3}-\text{Zr}^{+3}$  ( $\text{Co}^{+2}$  is the donor of electrons for  $\text{Zr}^{+4}$ ), in which  $\text{Co}^{+3}$  stabilizes  $\text{Zr}^{+3}$ . The presence of  $\text{Zr}^{+3}$  paramagnetic ions in the NZP catalysts was noted in [12].

The formation of two products, isobutylene (the main product) and isobutanol, is observed in the transformations of isobutanol over the Ni(Co)-CZP catalysts, which indicates two routes for alcohol transformation. Isobutylene is the most valuable product,

which is of interest for the polymer industry. It was found that the activity of triple CZP, like that of triple NZP, is higher than the activity of the double phosphate. Under our experimental conditions the total conversion of alcohol over the  $\text{CsZr}_2(\text{PO}_4)_3$  catalyst is below 25%; however, the isobutylene selectivity is 100%.

The conversion of isobutanol increases upon transition to the cooling mode; as a result, olefin selectivity decreases except for  $\text{Co}_{0.25}$  at 593 K and  $\text{Ni}_{0.25}$  at 653 K (Fig. 3). This means that an increase in the total conversion is associated with the formation of aldehyde, that is, intensification of the dehydrogenating function of the catalyst with sites involved in the redox process. The dehydrating function predominates in the Ni(Co)-CZP catalysts—the conversion of alcohol to isobutylene is substantially higher than the conversion of alcohol to isobutanol. This effect is especially pronounced in the samples with  $x = 0.15$  (Figs. 3, 4). As opposed to Ni(Co)-NZP, there is no clear break (manifestation of the M1  $\rightarrow$  M2 transition) in the dependences  $\ln N-T^{-1}$  in the transformations of isobutanol over the Ni(Co)-CZP catalysts (Fig. 4c), possibly, because of a larger radius of the  $\text{Cs}^+$  ion ( $r_{\text{Cs}^+} = 0.166$  nm versus  $r_{\text{Na}^+} = 0.098$  nm [13]).

The activity in the dehydration reaction of alcohol decreases upon transition to the cooling mode, and the activation energy increases (Table 3). Differences in the activation energies of olefin formation  $\Delta E^{\text{C=C}}$  increase with the concentration of  $\text{M}_x$  due to a decrease in  $E_a\uparrow$  because the values of  $E_a\downarrow$  are close and fall within 86–99 kJ/mol. An opposite character of changes in  $E_a$  and  $\ln N_0$  is observed in the case of the dehydrogenation reaction: the active state of the sites in the mode of decreasing temperature is characterized by a decrease in  $E_a^{\text{C=O}}$  with a small divergence of  $\Delta E^{\text{C=O}} = 55$  kJ/mol in the sample with  $\text{Co}_{0.15}$ .

A counter-clockwise thermal hysteresis (type I) was observed in the reaction of isobutanol dehydrogenation, and a clockwise thermal hysteresis (type II) was observed in the reaction of isobutanol dehydration; i.e., the catalytic processes differing in mechanisms and products have different types of hysteresis over the same catalyst. A change in the Arrhenius parameters in the case of hysteresis is affected by the amount of the dopant ion and its nature. The positive values of  $\Delta E^{\text{C=C}}$  increase in the order  $\text{Co}_{0.15} < \text{Co}_{0.25} < \text{Ni}_{0.15} < \text{Ni}_{0.25}$ . The negative values of  $\Delta E^{\text{C=O}}$  increase in the same order. Little attention is paid in the literature to the discussion of the thermal hysteresis of catalytic reactions within the framework of variability of the chemical composition and structure of the active site of a catalyst in the heating–cooling cycle due to the complexity of recording such changes. The thermal hysteresis was described for the oxidation reactions of CO and alkanes over oxide and supported catalysts [14–16]. In [14], the theoretical analysis of the

<sup>1</sup> J. Emsley, *The Elements*, 2nd ed. (Oxford Univ. Press, Oxford, 1991; Mir, Moscow, 1993).

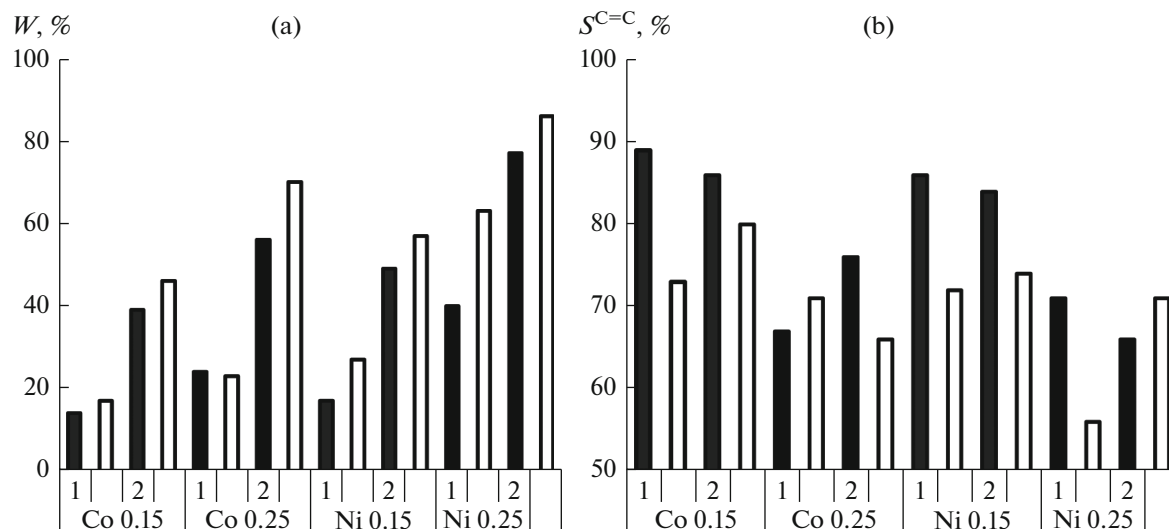


**Fig. 3.** (a) Total conversion of isobutanol and (b) isobutylene selectivity over the  $\text{Cs}_{(1-2x)}\text{M}_x\text{Zr}_2(\text{PO}_4)_3$  catalysts, where  $\text{M} = \text{Co}$  and  $\text{Ni}$ , at (1) 593 and (2) 653 K in the mode of heating (dark columns) and cooling (light columns).

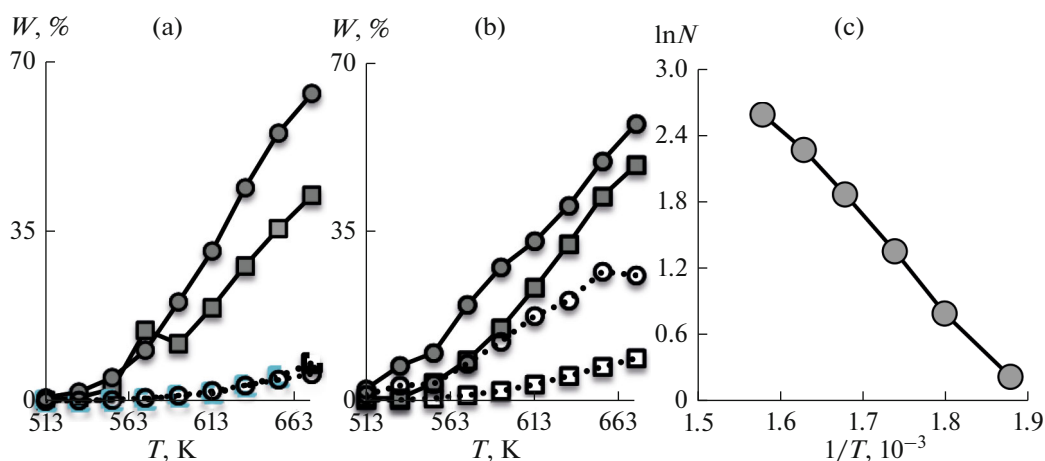


**Fig. 4.** (a, b) Temperature dependences of isobutanol conversion to isobutene (solid lines) and isobutanal (dashed lines) over  $\text{M}_x\text{-CZP}$  samples with (a)  $\text{Co}$  and (b)  $\text{Ni}$  for  $x = 0.15$  (squares) and  $0.25$  (circles) and (c) the Arrhenius dependence of isobutylene yield for  $x_{\text{Co}} = 0.25$ .

hysteresis of the partial oxidation reaction of methane  $\text{CH}_4 + \frac{1}{2}\text{O}_2 = \text{CO} + 2\text{H}_2$  ( $\Delta H = -36$  kJ/mol) was performed using the Reynolds and Damköhler numbers and taking into account the indirect mechanism, including three more reactions:  $\text{CH}_4 + 2\text{O}_2 = \text{CO}_2 + 2\text{H}_2\text{O}$  ( $\Delta H = -803$  kJ/mol),  $\text{CH}_4 + \text{H}_2\text{O} \leftrightarrow \text{CO} + 3\text{H}_2$  ( $\Delta H = +206$  kJ/mol), and  $\text{CH}_4 + \text{CO}_2 \leftrightarrow 2\text{CO} + 2\text{H}_2$  ( $\Delta H = +247$  kJ/mol). The authors [15] observed the thermal hysteresis in the co-oxidation reaction of  $\text{CO}$  and  $\text{C}_2\text{H}_6$  over a  $\text{Pt}/\text{Al}_2\text{O}_3$  catalyst at 300–600 K, which, in their opinion, differs from the thermal hysteresis of stationary activity. The thermal counter-clockwise hysteresis in the catalytic combustion (complete oxidation) of methane over  $\text{Pt}/\text{Al}_2\text{O}_3$  in a flow-

type reactor was analyzed in [16]. Using the new in situ obtained data the authors replaced the earlier explanation of the hysteresis by the removal of adsorbed oxygen from the  $\text{Pt}$  sites and their local warmup with another one—the formation of active carbon sites upon the dissociative adsorption of methane.

Thus, the often-observed thermal hysteresis of the activity of heterogeneous catalysts has not been unambiguously explained yet. Thermal hysteresis also takes place in the transformations of isopropanol and isobutanol over  $\text{Co}(\text{Ni})\text{-NZP}$  and  $\text{Co}(\text{Ni})\text{-CZP}$  complex phosphate catalysts with the NASICON structure. The counter-clockwise (type I) or clockwise (type II) type of hysteresis with a change in the activation

**Table 3.** Characteristics of isobutanol transformations over  $\text{Cs}_{(1-2x)}\text{M}_x\text{Zr}_2(\text{PO}_4)_3$ : the experimental activation energy for the formation of isobutylene  $E_a^{\text{C=C}}$  and isobutanal  $E_a^{\text{C=O}}$  in the mode of heating (numerator) and cooling (denominator) and changes in the activation energy

$M_x$	Dehydration of alcohol			Dehydrogenation of alcohol		
	$E_a^\uparrow/E_a^\downarrow$	$\Delta E_a^{\text{C=C}}, \text{kJ/mol}$	$\Delta \ln N_0^{\text{C=C}}$	$E_a^\uparrow/E_a^\downarrow$	$\Delta E_a^{\text{C=O}}, \text{kJ/mol}$	$\Delta \ln N_0^{\text{C=O}}$
$\text{Co}_{0.15}$	87/90	+3	+1	112/57	-55	-10
$\text{Co}_{0.25}$	61/91	+30	+6	74/47	-27	-6
$\text{Ni}_{0.15}$	57/99	+22	+9	67/48	-19	-3
$\text{Ni}_{0.25}$	33/86	+53	+11	69/48	-21	-4

energy and the preexponential factor depends on the composition of NZP (the conducting ion and dopant ion  $M^{+2} = \text{Co}, \text{Ni}$ ), reaction type (alcohol dehydrogenation or dehydration), and the range of reaction temperatures because M can occupy position M1 or M2 in the conductance channel of the solid electrolyte depending on temperature.

#### ACKNOWLEDGMENTS

We are grateful to the Shared Research Center Diagnostics of the Structure and Properties of Nanomaterials of the Belgorod State National Research University and personally to Dr. Sci. (Chem.) O.E. Lebedeva for her help in the study of Ni(Co)-NZP by X-ray diffractometry, scanning ion-electron spectroscopy, and nitrogen thermal desorption; to the Shared Research Center of the Moscow State University and personally to Cand. Sci. (Chem.) S.V. Savilov for his help in measuring the surface area, pore size, and X-ray photoelectron spectra of Ni(Co)-CZP samples; and to the Shared Research Center Physicochemical Studies of New Materials and Catalyst Systems of the Peoples' Friendship University of Russia and personally to Cand. Sci. (Chem.) N.N. Lobanov for the X-ray powder diffraction analysis of Ni(Co)-CZP samples.

#### FUNDING

Preparation of this publication was supported by the Program 5-100 of the Peoples' Friendship University of Russia.

#### CONFLICT OF INTEREST

The authors declare that there is conflict of interest to be disclosed in this paper.

#### ADDITIONAL INFORMATION

I.I. Mikhaleiko, ORCID: <https://orcid.org/0000-0002-5406-1015>

A.I. Pylinina, ORCID: <https://orcid.org/0000-0002-8190-6167>

E.I. Knyazeva, ORCID: <https://orcid.org/0000-0001-6254-0959>

#### REFERENCES

- J. Alamo, *Solid State Ionics* **63–65**, 547 (1993). [https://doi.org/10.1016/0167-2738\(93\)90158-Y](https://doi.org/10.1016/0167-2738(93)90158-Y)
- B. E. Scheetz, D. K. Agrawal, E. Breval, and R. Roy, *Waste Manag.* **14** (6), 489 (1994). [https://doi.org/10.1016/0956-053X\(94\)90133-3](https://doi.org/10.1016/0956-053X(94)90133-3)
- V. I. Pet'kov, *Russ. Chem. Rev.* **81** (7), 606 (2012). <https://doi.org/10.1070/RC2012v081n07ABEH004243>
- Sh. Zhang, B. Quan, Zh. Zhao, B. Zhao, Y. He, and W. Chen, *Mater. Lett.* **58** (1–2), 226 (2004). [https://doi.org/10.1016/S0167-577X\(03\)00450-6](https://doi.org/10.1016/S0167-577X(03)00450-6)
- S. Arsalane, M. Kacimi, M. Ziyad, G. Coudurier, and J. C. Vedrine, *Appl. Catal., A* **114** (2), 243 (1994). [https://doi.org/10.1016/0926-860X\(94\)80177-0](https://doi.org/10.1016/0926-860X(94)80177-0)
- S. N. Pavlova, V. A. Sadykov, E. A. Paukshtis, E. B. Burgina, S. P. Degtyarev, D. I. Kochubei, A. V. Kalinkin, N. F. Saputina, R. I. Maximovskaya, V. I. Zaikovskii, R. Roy, and D. Agrawal, in *Studies in Surface Science and Catalysis*, Ed. by A. Parmaliana, D. Sanfilippo, F. Frusteri, A. Vaccari, and F. Arena (Elsevier Science B.V.: Amsterdam, 1998), **Vol. 119**, pp. 759–764. [https://doi.org/10.1016/S0167-2991\(98\)80523-5](https://doi.org/10.1016/S0167-2991(98)80523-5)
- M. M. Ermilova, M. V. Sukhanov, R. S. Borisov, N. V. Orekhova, V. I. Pet'kov, S. A. Novikova, A. B. Il'in, and A. B. Yaroslavtsev, *Catal. Today* **193** (1), 37 (2012). <https://doi.org/10.1016/j.cattod.2012.02.029>
- A. B. Ilyin, M. M. Ermilova, N. V. Orekhova, and A. B. Yaroslavtsev, *Nanotechnol. Russ.* **13** (7–8), 365 (2018). <https://doi.org/10.1134/S1995078018040067>
- E. I. Povarova, A. I. Pylinina, and I. I. Mikhaleiko, *Rus. J. Phys. Chem. A* **86** (6), 935 (2012). <https://doi.org/10.1134/S0036024412060210>

10. E. I. Povarova, A. I. Pylinina, and I. I. Mikhalenko, *Prot. Met. Phys. Chem. Surf.* **50** (3), 331 (2014).  
<https://doi.org/10.1134/S2070205114030125>
11. A. I. Pylinina, M. N. Chernyshova, N. N. Lobanov, S. V. Savilov, and E. M. Kasatkin, *Theor. Exp. Chem.* **53** (1), 47 (2017).  
<https://doi.org/10.1007/s11237-017-9500-3>
12. S. Arsalane, M. Ziyad, G. Coudurier, and J. C. Vedrine, *J. Catal.* **159** (1), 162 (1996).  
<https://doi.org/10.1006/jcat.1996.0075>
13. L. T. Bugaenko, S. M. Ryabykh, and A. L. Bugaenko, *Moscow Univ. Chem. Bull.* **63** (6), 363 (2008).  
<https://doi.org/10.3103/S0027131408060011>
14. W.-H. Chen, T.-W. Chiu, and C.-I. Hung, *Int. J. Hydrogen Energy* **35** (12), 6291 (2010).  
<https://doi.org/10.1016/j.ijhydene.2010.03.133>
15. R. K. Dadi, D. Luss, and V. Balakotaiah, *Chem. Eng. J.* **297**, 325 (2016).  
<https://doi.org/10.1016/j.cej.2016.03.139>
16. L. Chen, J. P. McCann, and S. L. Tait, *Appl. Catal., A* **549**, 19 (2018).  
<https://doi.org/10.1016/j.apcata.2017.09.008>

*Translated by E. Boltukhina*